Trajectory Planning and Tracking Control of Underactuated AUVs*

Filoktimon Repoulias and Evangelos Papadopoulos
Department of Mechanical Engineering, National Technical University of Athens, 15780 Athens, Greece
firepoul@central.ntua.gr, egpapado@central.ntua.gr

Abstract– **This paper addresses the combined problem of trajectory planning and tracking control for underactuated AUVs moving on the horizontal plane. A reference feasible trajectory for the position and orientation of the AUV is planned so that it is consistent with vehicle dynamics. Using these reference values the dynamics of the vehicle is transformed to the error one. Partial state-feedback linearization, backstepping and non-linear damping techniques are utilized to stabilize the above system and force the tracking error to a neighborhood about zero that can be made arbitrarily small. Simulation results that validate the proposed tracking methodology are presented and discussed.**

***Index Terms–* trajectory planning, underactuated AUV tracking.**

I. Introduction

Autonomous Underwater Vehicles (AUVs), Fig. 1, are playing a crucial role in exploration and exploitation of resources located at deep oceanic environments. They are employed in risky missions such as oceanographic observations, bathymetric surveys, ocean floor analysis, military applications, recovery of lost man-made objects, etc., [1]. Besides their numerous practical applications, these vehicles present a challenging control problem when they are underactuated, i.e., they have fewer inputs than degrees of freedom. Such a control configuration imposes nonintegrable acceleration constraints. In addition, AUVs' kinematic and dynamic models are highly nonlinear and coupled, [2], making control design a hard task. Underactuation rules out the use of trivial control designs e.g. full state-feedback linearization, [3], and the complex hydrodynamics excludes designs based only on the kinematic model. When moving on a horizontal plane, AUVs present similar dynamic behavior to underactuated surface vessels, [4].

The stabilization problem, i.e. regulation to a point with a desired orientation, for surface vessels and AUVs has been studied in [4], [5], [6], [7], [8], [9]. It is shown that such vehicles cannot be asymptotically stabilized by continuous time-invariant feedback control laws.

Trajectory tracking deals with the design of control laws that force the vehicle to reach and track a time parameterized inertial trajectory, (a space curve with an associated timing law) [15].

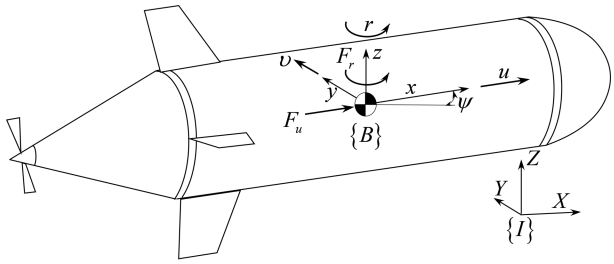

Fig. 1. Underactuated AUV and motion variables.

Tracking controller designs for underactuated marine vehicles currently in use follow classical approaches such as local linearization and decoupling of the multivariable model to steer as many degrees of freedom as the available control inputs. This is done using standard linear (or nonlinear) methods, [2]. Other approaches include the linearization of the vehicle's error dynamics about trimming trajectories that lead to time invariant linear systems followed by such techniques as gain scheduling, [10]. The validity of these solutions is limited in a small neighborhood around the selected operating points. Stability and performance also suffer significantly when the vehicle executes maneuvers that emphasize the action of its complex hydrodynamics and nonlinear coupling terms.

Theoretical and experimental results on trajectory tracking for underactuated marine vehicles show that nonlinear Lyapunov-based techniques can overcome most of the limitations mentioned above. The authors in [11] and [12], present experimental tracking results for a model ship using Lyapunov-based controllers. In [13], two tracking solutions for a surface vessel were proposed, based on Lyapunov's direct method and passivity approach. However, in the last three works, the yaw velocity was required to be nonzero. Under this restriction straight lines cannot be tracked. In [14], the error dynamics is transformed into a skew-symmetric form and practical convergence is achieved. The authors in [15] have designed a controller for vehicles moving in two or three dimensions that exponentially forces the position tracking error to a small neighborhood of the origin. However, the attitude of the vehicle is left uncontrolled, which may lead to undesirable backward tracking of the trajectory.

In this paper, the combined problem of trajectory

*Support of this work by the NTUA Senator Committee of Basic Research, Programme "Protagoras", R.C. No. 10, is acknowledged.

planning and tracking control for underactuated AUVs moving on the horizontal plane is addressed. The reference trajectory, consisting of the desired inertial position and the corresponding velocities, is designed to be a feasible "state-space" trajectory i.e. consistent with the vehicle dynamics. Based on the dynamics and the reference velocities, the reference orientation is also computed. The trajectory is required to be three times differentiable with respect to time. Using the resulting reference trajectory, the vehicle error dynamics is obtained and the control problem reduces to error dynamics stabilization. To this end, methods such as partial state-feedback linearization, backstepping, and nonlinear damping, [16], are used to design a time varying control law that forces the tracking error to a neighborhood of zero that can be reduced arbitrarily. A natural requirement in the above design is that the surge velocity is nonzero. Simulation results that validate the above design are presented and discussed.

II. Kinematic and Dynamic Model

In this section, the kinematic and dynamic equations of the motion of an AUV moving on the horizontal plane are described. Using an inertial reference frame $\{I\}$ and a body-fixed frame $\{B\}$, Fig. 1, the kinematic equations of motion of the center of mass (CM) for an AUV on the horizontal $X-Y$ plane can be written as [2]:

$$\dot{x} = u\cos\psi - \upsilon\sin\psi \tag{1a}$$

$$\dot{y} = u\sin\psi + \upsilon\cos\psi \tag{1b}$$

$$\dot{\psi} = r \tag{1c}$$

where x and y represent the inertial coordinates of the CM of the vehicle and u, υ are the surge and sway velocities respectively defined in the body-fixed frame, see Fig. 1. The orientation of the vehicle is described by the angle ψ and r is its yaw (angular) velocity. Assuming that i) the origin of the body-fixed reference frame coincides with the CM and the center of buoyancy, ii) the mass distribution is homogeneous, iii) the hydrodynamic damping terms of order higher than one are negligible, and iv) the heave, pitch, and roll motions can be neglected, the dynamics for a neutrally buoyant torpedo shaped AUV is expressed by the following differential equations [2]:

$$\dot{u} = \frac{m_{22}}{m_{11}}\upsilon r - \frac{d_{11}}{m_{11}}u + \frac{1}{m_{11}}F_u \tag{2a}$$

$$\dot{\upsilon} = -\frac{m_{11}}{m_{22}}ur - \frac{d_{22}}{m_{22}}\upsilon \tag{2b}$$

$$\dot{r} = \frac{m_{11}-m_{22}}{m_{33}}u\upsilon - \frac{d_{33}}{m_{33}}r + \frac{1}{m_{33}}F_r \tag{2c}$$

where the constants m_{11}, m_{22}, and m_{33} represent the combined inertia and added mass terms, and the constants d_{11}, d_{22}, and d_{33} represent the hydrodynamic damping terms. The variable F_u denotes control force along the surge motion of the vehicle and F_r denotes control torque that is applied in order to produce angular motion around the z axis of the body-fixed frame. There is no side thruster to create sway motion; therefore (2b) is uncontrolled and the vehicle an underactuated dynamical system. The above control configuration can be realized e.g. by providing the vehicle with two horizontal stern propellers or with a stern propeller and a rudder, Fig. 1.

III. Trajectory Planning

This section, describes the reference trajectory planning methodology. The only restriction on this trajectory is that it must be sufficiently "smooth", i.e., a continuous curve and three times differentiable with respect to time.

A. Path kinematics

Let us assume that for the tracking control problem the planar path that must be tracked by the CM of an AUV is given as a time function of the inertial variables $x_R(t), y_R(t)$. Taking their time derivatives, we also compute the corresponding velocities and accelerations $\dot{x}_R(t), \dot{y}_R(t), \ddot{x}_R(t), \ddot{y}_R(t)$. The subscript "R" indicates a reference variable. (In the remainder of the paper, time dependence notation is omitted). The magnitude of the velocity vector $\mathbf{v}_p$ of a point on the path at time t is given by

$$v_p = \|\mathbf{v}_p\| = \|[\dot{x}_R, \dot{y}_R]^T\| = \sqrt{\dot{x}_R^2 + \dot{y}_R^2} \tag{3}$$

The direction of $\mathbf{v}_p$ is given by the angle β, see Fig. 2:

$$\beta = \tan^{-1}\left(\dot{y}_R / \dot{x}_R\right) \tag{4}$$

The time variation of the direction and of the magnitude of the velocity vector are respectively given by

$$\omega = \dot{\beta} = (\dot{x}_R\ddot{y}_R - \dot{y}_R\ddot{x}_R) / (\dot{x}_R^2 + \dot{y}_R^2) \tag{5}$$

$$\dot{v}_p = (\dot{x}_R\ddot{x}_R + \dot{y}_R\ddot{y}_R) / (\sqrt{\dot{x}_R^2 + \dot{y}_R^2}) \tag{6}$$

B. Vehicle's Dynamics on the Path

The procedure for determining the algebraic and differential equations that relate the reference trajectory variables to the vehicle states follows. Considering the dynamics of the AUV as it tracks the reference trajectory, let u_R, υ_R, r_R denote the body-fixed velocities. Thus, the magnitude of the velocity vector of the CM is

$$v_R = \|\mathbf{v}_R\| = \|[u_R, \upsilon_R]^T\| = \sqrt{u_R^2 + \upsilon_R^2} \tag{7}$$

As far as the reference orientation ψ_R -the angle between the inertial X axis and the body x axis- is concerned, the following is observed (see Fig. 2): when the vehicle tracks a generic planar path (with nonzero curvature), vector $\mathbf{v}_R$ must be tangent to the path. As a result, ψ_R doesn't coincide with the angle between $\mathbf{v}_R$ and the inertial X

axis but it differs by some angle γ. The latter is created as a consequence of the dynamics of the vehicle as this rotates. Specifically, looking at (2b) and considering that the CM of the vehicle tracks the path, we see that because of surge and yaw motions, the coupling term $u_R r_R$ gives rise to a sway motion υ_R. A direct result is the appearance of γ which is expressed as

$$\gamma = \tan^{-1}(\upsilon_R / u_R) \tag{8}$$

Having the description of the path and the states of the AUV as it tracks the path, we conclude that the following geometric conditions must hold: Firstly, the magnitude of the tangent vector to the path $\mathbf{v}_p$ equals the magnitude of the vehicle's velocity vector $\mathbf{v}_R$. From (3) and (7) it is:

$$v_p = v_R \Rightarrow \sqrt{\dot{x}_R^2 + \dot{y}_R^2} = \sqrt{u_R^2 + \upsilon_R^2} \tag{9}$$

Secondly, observing Fig. 2 and taking into account (4) and (8), the relationship between the various angles is

$$\psi_R = \beta \pm \gamma = \tan^{-1}(\dot{y}_R / \dot{x}_R) \pm \tan^{-1}(\upsilon_R / u_R) \tag{10}$$

In (10), the sign "$\pm$" depends on the curvature of the trajectory, i.e. a plus sign corresponds to a counterclockwise rotation and the minus sign to an opposite one. From (9) and (3), the reference sway velocity is

$$\upsilon_R = \pm\sqrt{\dot{x}_R^2 + \dot{y}_R^2 - u_R^2} = \pm\sqrt{v_p^2 - u_R^2} \tag{11}$$

where "$\pm$" indicates that υ_R may be positive or negative depending on path curvature. If $u_R > 0$ and $r_R > 0$, then $\upsilon_R < 0$. Differentiating (11) yields

$$\dot{\upsilon}_R = \pm(v_p \dot{v}_p - u_R \dot{u}_R) \big/ (\sqrt{v_p^2 - u_R^2}) \tag{12}$$

where $\dot{v}_p$ is given by (6). Also from (11) it is

$$-v_p \le u_R \le v_p \tag{13}$$

where the equality holds in the case of straight line tracking or when a change in the sign of the curvature occurs (then $\upsilon_R = r_R = 0$). The reference angular velocity that corresponds to the path is obtained by differentiating ψ_R in (10) and taking into account (5), (6) and (11):

$$r_R = \dot{\psi}_R = \omega \pm [(u_R \dot{v}_p - \dot{u}_R v_p) \big/ (v_p \sqrt{v_p^2 - u_R^2})] \tag{14}$$

By substituting expressions (12), (11), and (14) that give $\dot{\upsilon}_R, \upsilon_R$, and r_R in (2b), the following differential equation results whose solution yields the reference surge velocity:

$$\begin{aligned} \dot{u}_R = &\left[1/u_R v_p (m_{11} - m_{22})\right](d_{22} u_R^2 v_p - d_{22} v_R^3 - \\ &m_{11} \omega u_R v_p \sqrt{v_p^2 - u_R^2} + m_{11} u_R^2 \dot{v}_p - m_{22} \dot{v}_p v_p^2),\ u_R(t=0) \ne 0 \end{aligned} \tag{15}$$

Finally, the required open-loop control force and torque are obtained from (2a) and (2c) as follows:

$$F_{uR} = m_{11}\dot{u}_R - m_{22}\upsilon_R r_R + d_{11} u_R \tag{16a}$$

$$F_{rR} = m_{33}\dot{r}_R + (m_{22} - m_{11}) u_R \upsilon_R + d_{33} r_R \tag{16b}$$

where $\dot{r}_R$ is obtained by differentiating (14).

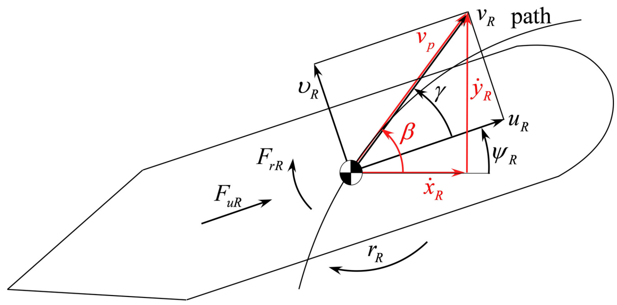

Fig. 2. An AUV moving along a planar path.

To illustrate the way the above methodology can be applied, consider as a reference planar trajectory a circle described by $x_R = 10\sin(0.01t)$ and $y_R = 10\cos(0.01t)$, in m. The corresponding first and second derivatives are $\dot{x}_R = 0.1\cos(0.01t)$, $\dot{y}_R = -0.1\sin(0.01t)$ in m/s, and $\ddot{x}_R = -0.1^2\sin(0.01t)$, $\ddot{y}_R = -0.1^2\cos(0.01t)$, in m/s^2. From (3) and (6) it is $v_p = 0.1\ m/s$ and $\dot{v}_p = 0$. Also from (5), it is $\omega = -0.01\ rad/s$ meaning a "clockwise" curve. Forward tracking of this circle requires the reference states of the AUV signed as $u_R > 0$, $\upsilon_R > 0$, and $r_R < 0$. Their values are computed as follows: in (15), we substitute v_p, $\dot{v}_p$, and ω for their previously computed values. We also substitute the constant terms for their numerical values taken from [7]. Solving numerically the resulting differential equation

$$\dot{u}_R = -(0.2/u_R)[10u_R^2 - 0.1 + 0.215 sqrt(0.01 - u_R^2) u_R] \tag{15'}$$

with $u_R(0) = 10^{-3}$, we obtain $u_R = 0.099$ and $\dot{u}_R = 0$. It is easy now, using (11), (12), and (14) with the appropriate substitutions, to obtain $\upsilon_R = 0.0021$, $\dot{\upsilon}_R = 0$, $r_R = -0.01$, and $\dot{r}_R = 0$ (SI units). Additionally, from (8) it is $\gamma = 1.23^\circ$ which means that the body x axis must point inside the circle during tracking. From (16), the open-loop control force and torque must be $F_{uR} = 7.004\ N$ and $F_{rR} = -0.488\ Nm$.

From the preceding trajectory planning methodology we conclude the following: The reference orientation ψ_R of the vehicle doesn't coincide with the angle between the velocity vector $\mathbf{v}_p$ and the X axis but it depends on the variables of the trajectory -time parameterization, differentiability, etc.- and the vehicle dynamics, (10). AUV dynamics plays also a crucial role in the kind of trajectories that can be tracked.

The above analysis holds when the vehicle is "on the path" i.e., position, orientation, and velocity errors are zero. In cases such as the vehicle starts away from the reference trajectory, or there are modeling errors or external disturbances, the open-loop control doesn't suffice; a closed-loop trajectory-tracking controller is needed to drive the vehicle to the reference trajectory and the corresponding errors to zero. This is discussed next.

IV. Trajectory Tracking Control Design

In this section, the trajectory-tracking control design is presented. We assume bounded reference body-fixed velocities and nonzero surge velocity.

A. Error dynamics formulation

Using the states of the vehicle and the previously computed reference variables, the tracking errors are defined as $u_e = u - u_R$, $\upsilon_e = \upsilon - \upsilon_R$, $r_e = r - r_R$, $x_e = x - x_R$, $y_e = y - y_R$, $\psi_e = \psi - \psi_R$. Substituting for u, υ, r, x, y, and ψ in (1) and (2) we obtain the error dynamics as follows. Firstly, from kinematics it is:

$$\begin{bmatrix} \dot{x}_e \\ \dot{y}_e \end{bmatrix} = \begin{bmatrix} \cos\psi & -\sin\psi \\ \sin\psi & \cos\psi \end{bmatrix} \begin{bmatrix} u_e \\ \upsilon_e \end{bmatrix} + \begin{bmatrix} \cos\psi - \cos\psi_R & -\sin\psi + \sin\psi_R \\ \sin\psi - \sin\psi_R & \cos\psi - \cos\psi_R \end{bmatrix} \begin{bmatrix} u_R \\ \upsilon_R \end{bmatrix} \quad (17a, b)$$

$$\dot{\psi}_e = r_e \quad (17c)$$

In a more compact form (17a, b) can be written as:

$$\dot{\mathbf{x}}_e = \mathbf{R}\mathbf{u}_e + \mathbf{R}_{\psi,\psi_R}\mathbf{u}_R \quad (18)$$

where $\mathbf{x}_e \triangleq [x_e, y_e]^T$, $\mathbf{u}_e \triangleq [u_e, \upsilon_e]^T$, $\mathbf{u}_R \triangleq [u_R, \upsilon_R]^T$, and

$$\mathbf{R}(\psi) = \mathbf{R} \triangleq \begin{bmatrix} \cos\psi & -\sin\psi \\ \sin\psi & \cos\psi \end{bmatrix} \quad (19a)$$

$$\mathbf{R}_{\psi,\psi_R} \triangleq \mathbf{R}(\psi) - \mathbf{R}(\psi_R) \quad (19b)$$

Then, considering dynamics we obtain

$$\dot{u}_e = \frac{m_{22}}{m_{11}}\left(\upsilon_e r_e + \upsilon_e r_R + \upsilon_R r_e\right) - \frac{d_{11}}{m_{11}} u_e + \frac{\left(F_u - F_{uR}\right)}{m_{11}} \quad (20a)$$

$$\dot{\upsilon}_e = -\frac{m_{11}}{m_{22}}\left(u_e r_e + u_e r_R + u_R r_e\right) - \frac{d_{22}}{m_{22}}\upsilon_e \quad (20b)$$

$$\dot{r}_e = \frac{m_{11} - m_{22}}{m_{33}}\left(u_e \upsilon_e + u_e \upsilon_R + u_R \upsilon_e\right) - \frac{d_{33}}{m_{33}} r_e + \frac{\left(F_r - F_{rR}\right)}{m_{33}} \quad (20c)$$

B. Error dynamics stabilization

The control objective now is to stabilize the error dynamics. Towards this, and taking

$$F_u = F_{uR} + d_{11}u_e - m_{22}(\upsilon_e r_e + \upsilon_e r_R + \upsilon_R r_e) + m_{11}\tau_u \quad (21)$$

$$F_r = F_{rR} + d_{33}r_e + (m_{22} - m_{11})(u_e\upsilon_e + u_e\upsilon_R + u_R\upsilon_e) + m_{33}\tau_r \quad (22)$$

yields a partial linearized system consisting of (17c), (18), (20b), along with the integrators

$$\dot{u}_e = \tau_u \quad (23)$$

$$\dot{r}_e = \tau_r \quad (24)$$

where τ_u and τ_r are auxiliary controls along the surge and yaw motions respectively. F_{uR} and F_{rR} are given in (16).

Next, backstepping and nonlinear damping are employed as our design tools, [16].

Step 1. Considering the subsystem (18), we take as virtual control the vector $\mathbf{u}_e = [u_e, \upsilon_e]^T$ and as a bounded disturbance (for bounded u_R and υ_R) the vector $\boldsymbol{\delta} \triangleq \mathbf{R}_{\psi,\psi_R}\mathbf{u}_R = [\delta_1, \delta_2]^T$. Choosing

$$V_1 = \mathbf{x}_e^T \mathbf{x}_e / 2 \quad (25)$$

the desired expressions for the virtual controls are

$$\mathbf{u}_{e,des} = -\mathbf{R}^T(\mathbf{K} + \mathbf{K}_1)\mathbf{x}_e \triangleq \boldsymbol{\alpha}(\mathbf{x}_e) = [\alpha_u, \alpha_\upsilon]^T \quad (26)$$

where $\mathbf{K} = diag(k, k)$ and $\mathbf{K}_1 = diag(k_1, k_1)$ are positive-definite gain matrices. The time derivative of (25) is:

$$\dot{V}_1 = -\mathbf{x}_e^T(\mathbf{K} + \mathbf{K}_1)\mathbf{x}_e + \mathbf{x}_e^T\boldsymbol{\delta} \le -\mathbf{x}_e^T\mathbf{K}\mathbf{x}_e + [(\delta_1^2 + \delta_2^2)/4k_1] \quad (27)$$

Increasing k_1, $(\delta_1^2 + \delta_2^2)/4k_1$ can be arbitrarily small.

Step 2. The components of the vector $\mathbf{u}_e = [u_e, \upsilon_e]^T$ are not true controls, thus we have to introduce appropriate error variables $\mathbf{z}_u = [z_u, z_\upsilon]^T = [u_e - \alpha_u, \upsilon_e - \alpha_\upsilon]^T$ in the controlled position equations as follows:

$$\dot{\mathbf{x}}_e = -(\mathbf{K} + \mathbf{K}_1)\mathbf{x}_e + \mathbf{R}\mathbf{z}_u + \boldsymbol{\delta} \quad (28a)$$

$$\dot{z}_u = \tau_u - \dot{\alpha}_u \quad (28b)$$

$$\dot{z}_\upsilon = -(m_{11}/m_{22})(u_e r_e + u_e r_R + u_R r_e) - (d_{22}/m_{22})\upsilon_e - \dot{\alpha}_\upsilon \quad (28c)$$

The task now is to stabilize the error variables z_u and z_υ. In this step, z_u is stabilized using τ_u. Choosing

$$V_2 = V_1 + z_u^2/2 \quad (29)$$

its time derivative becomes

$$\dot{V}_2 = \mathbf{x}_e^T[-(\mathbf{K} + \mathbf{K}_1)\mathbf{x}_e + \mathbf{R}\mathbf{z}_u + \boldsymbol{\delta}] + z_u[\tau_u - \dot{\alpha}_u] \quad (30)$$

Utilizing (27), and after some straightforward algebraic manipulations, (30) becomes

$$\begin{aligned} \dot{V}_2 \le & -\mathbf{x}_e^T\mathbf{K}\mathbf{x}_e + [(\delta_1^2 + \delta_2^2)/4k_1] + x_e(z_u\cos\psi \\ & - z_\upsilon\sin\psi) + y_e(z_u\sin\psi + z_\upsilon\cos\psi) + \\ & z_u[\tau_u + (k + k_1)u_e + (k + k_1)(\delta_1\cos\psi + \delta_2\sin\psi)] \end{aligned} \quad (31)$$

Young's inequality [3], for a positive k_2, gives

$$\begin{aligned} & x_e(z_u\cos\psi - z_\upsilon\sin\psi) + y_e(z_u\sin\psi + z_\upsilon\cos\psi) \\ & < k_2(x_e^2 + y_e^2) + [(z_u^2 + z_\upsilon^2)/4k_2] \end{aligned} \quad (32)$$

and (31) becomes

$$\begin{aligned} \dot{V}_2 \le & -(k - k_2)x_e^2 - (k - k_2)y_e^2 + [(\delta_1^2 + \delta_2^2)/4k_1] \\ & + [(z_u^2 + z_\upsilon^2)/4k_2] + z_u[\tau_u + (k + k_1)u_e + \\ & (k + k_1)(\delta_1\cos\psi + \delta_2\sin\psi)] \end{aligned} \quad (33)$$

Choosing $k > k_2$ the first two terms become nonpositive. The fourth term is discussed in the next steps. Setting

$$\tau_u = -(k + k_1)u_e - c_u z_u - k_u z_u (k + k_1)^2(\cos^2\psi + \sin^2\psi) \quad (34)$$

with k_u, $c_u > (1/4k_2)$ positive constants, and doing the algebra, (33) becomes

$$\begin{aligned} \dot{V}_2 \le & -(k - k_2)x_e^2 - (k - k_2)y_e^2 - c_u z_u^2 + \\ & [(1/4k_1) + (1/4k_u)](\delta_1^2 + \delta_2^2) + [(z_u^2 + z_\upsilon^2)/4k_2] \\ = & -(k - k_2)x_e^2 - (k - k_2)y_e^2 - [c_u - (1/4k_2)]z_u^2 + \\ & [(1/4k_1) + (1/4k_u)](\delta_1^2 + \delta_2^2) + [(z_\upsilon^2)/4k_2] \end{aligned} \quad (35)$$

Step 3. The next subsystem to stabilize consists of (17c), and (28c) which is rewritten as

$$\dot{z}_\upsilon = -(m_{11}/m_{22})ur_e + \delta_\upsilon \tag{36}$$

where

$$\begin{aligned}\delta_\upsilon &= -(m_{11}/m_{22})u_e r_R + [k + k_1 - (d_{22}/m_{22})]\upsilon_e \\ &\quad + (k + k_1)(\delta_2 \cos\psi - \delta_1 \sin\psi)\end{aligned} \tag{37}$$

The above term is bounded provided that u_e and υ_e are bounded. This is achieved once the complete system controller is designed at the final step. Considering the error $r_e = \alpha_r$ as virtual control, assuming $u \neq 0$, choosing

$$V_3 = V_2 + \left(z_\upsilon^2 + \psi_e^2\right)/2 \tag{38}$$

and taking into account (35), it is

$$\dot{V}_3 \le W + b + z_\upsilon[-(m_{11}/m_{22})u\alpha_r + \delta_\upsilon] + \psi_e \alpha_r + [(z_\upsilon^2)/4k_2] \tag{39}$$

where $b = [(1/4k_1) + (1/4k_u)](\delta_1^2 + \delta_2^2)$ can be made arbitrarily small. We also have made the substitution $W = -(k - k_2)x_e^2 - (k - k_2)y_e^2 - [c_u - (1/4k_2)]z_u^2$. Setting

$$\alpha_r = -c_r[-(m_{11}/m_{22})uz_\upsilon + \psi_e] \tag{40}$$

for some c_r positive, (39) becomes

$$\begin{aligned}\dot{V}_3 &\le W + b - c_r(m_{11}uz_\upsilon/m_{22})^2 - c_r\psi_e^2 + z_\upsilon\delta_\upsilon \\ &\quad + 2c_r(m_{11}/m_{22})uz_\upsilon\psi_e + (z_\upsilon^2/4k_2)\end{aligned} \tag{41}$$

For some positive k_z, k_ψ Young's inequality gives

$$z_\upsilon\delta_\upsilon < k_z z_\upsilon^2 + (\delta_\upsilon^2/4k_z) \tag{42a}$$

$$2c_r\left(m_{11}/m_{22}\right)uz_\upsilon\psi_e < k_\psi z_\upsilon^2 + [(c_r m_{11}u\psi_e/m_{22})^2/k_\psi] \tag{42b}$$

Thus, (41) becomes

$$\begin{aligned}\dot{V}_3 &\le W + b - c_r\psi_e^2 + (\delta_\upsilon^2/4k_z) - [c_r(m_{11}u/m_{22})^2 \\ &\quad - (k_z + k_\psi + (1/4k_2))]z_\upsilon^2 + (c_r^2/k_\psi)(m_{11}u\psi_e/m_{22})^2\end{aligned} \tag{43}$$

Step 4. The variable r_e is not a true control. Thus, we have to introduce an error $z_r = r_e - \alpha_r$ and use τ_r:

$$\dot{z}_\upsilon = -(m_{11}u/m_{22})(\alpha_r + z_r) + \delta_\upsilon \tag{44a}$$

$$\dot{\psi}_e = \alpha_r + z_r \tag{44b}$$

$$\dot{z}_r = \tau_r - \dot{\alpha}_r \tag{44c}$$

Using (43) and choosing

$$V_4 = V_3 + z_r^2/2 \tag{45}$$

we have

$$\begin{aligned}\dot{V}_4 &\le W + b - c_r\psi_e^2 + (\delta_\upsilon^2/4k_z) - [c_r(m_{11}u/m_{22})^2 \\ &\quad - (k_z + k_\psi + (1/4k_2))]z_\upsilon^2 + (c_r^2/k_\psi)(m_{11}u\psi_e/m_{22})^2 \\ &\quad + z_r[\tau_r + z_\upsilon + \psi_e + c_r[(m_{11}u/m_{22})^2 + 1]r_e \\ &\quad - c_r(m_{11}u/m_{22})\delta_\upsilon]\end{aligned} \tag{46}$$

With positive c and k_c, and taking

$$\begin{aligned}\tau_r &= -z_\upsilon - \psi_e - c_r[(m_{11}u/m_{22})^2 + 1]r_e \\ &\quad - [c + k_c(c_r m_{11}u/m_{22})^2]z_r\end{aligned} \tag{47}$$

and after some manipulations, (46) becomes

$$\begin{aligned}\dot{V}_4 &\le W + b - [c_r - ((c_r m_{11}u)^2/m_{22}^2 k_\psi)]\psi_e^2 - \\ &\quad [c_r(m_{11}u/m_{22})^2 - (k_z + k_\psi + k_3((m_{11}u/m_{22})^2 + 1) \\ &\quad + (1/4k_2))]z_\upsilon^2 - [c - (1/4k_3)]z_r^2 - k_c[z_r c_r \\ &\quad (m_{11}u/m_{22}) + (\delta_\upsilon/2k_c)]^2 + [(1/4k_z) + (1/4k_c)]\delta_\upsilon^2\end{aligned} \tag{48}$$

The third and fourth terms must be negative definite. This gives a system of two inequalities the compatibility of which provides the range of the values of c_r. The term $[(1/4k_z) + (1/4k_c)]\delta_\upsilon^2$ is bounded and can be made arbitrarily small increasing the gains k_z or k_c. Also $c > (1/4k_3)$. Setting

$$\Delta = b + [(1/4k_z) + (1/4k_c)]\delta_\upsilon^2 \tag{49}$$

we can conclude that there is a positive constant ξ, sufficiently small, such that

$$\dot{V}_4 \le -\xi V_4 + \Delta \tag{50}$$

Utilizing the Comparison Lemma [3], we conclude that

$$V_4 \le e^{-\xi t}V_4(0) + (\Delta/\xi) \tag{51}$$

meaning that the states of the error dynamics remain in a bounded set around zero. At this result we arrived using the controls in (21), and (22), along with (34), and (47).

V. Simulation Results

A large number of simulation results showed that the above designed controls perform very well in terms of quick convergence of the tracking errors to zero, smooth transient response, low control effort, and robustness, even in the case of large initial errors. To illustrate the performance of the proposed trajectory planning and tracking control methods, typical simulation results are presented.

The desired circular trajectory used in Section III and the corresponding reference body-fixed velocities and orientation are used here again. The dynamic model in (2) is the same as well. The following results were obtained with controller gains chosen as: $k = c_u = 0.5$, $k_1 = k_u = 0.7$, $c_r = 0.1$, and $c = k_c = 0.6$. The underactuated vehicle starts from rest, meaning initial velocity errors are $|u_e| = 0.099\ m/s$, $|\upsilon_e| = 0.0021\ m/s$, and $|r_e| = 0.01\ rad/s$, and the initial position and orientation errors are $|x_e| = 0.5\ m$, $|y_e| = 1\ m$, and $|\psi_e| = 20^\circ$. In Fig. 3, the reference and the resulting trajectory of the CM of the AUV in the inertial $X - Y$ plane are displayed. Fig. 4, shows the control force F_u and the control torque F_r needed for tracking. After a short period of time -needed for the errors to converge to a neighborhood of zero- they converge smoothly, see Fig. 4(b, d), to their open-loop values, given by (16). The errors in velocities are depicted in Fig. 5(a, b, c, d, e, f). After a short time period of transition, they converge smoothly to a neighborhood of zero, of the order of $10^{-5}\ m/s$ or rad/s, and slowly oscillate within. In Fig. 6(a, b, c, d, e, f), the tracking errors in position and orientation are depicted. Again, after a smooth transition period the errors converge and remain to a small neighborhood of zero of the order of $10^{-5} m$ or deg, verifying the theoretical results.

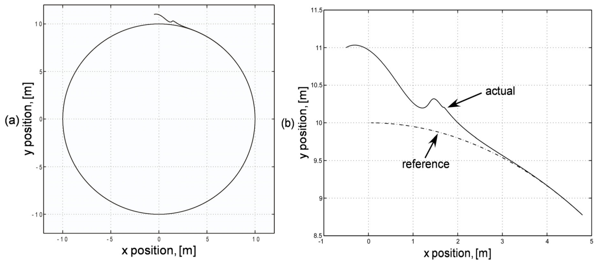

Fig. 3. (a) AUV reference and actual path. (b) First 50 s.

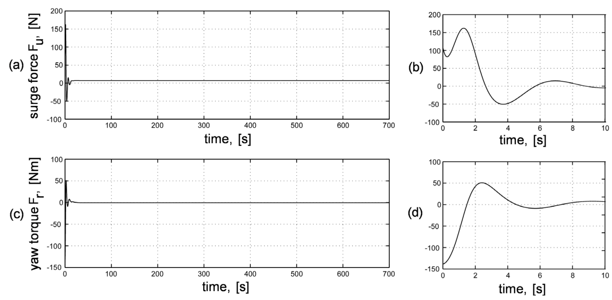

Fig. 4. (a), (c) Control surge force & yaw torque. (b), (d) First 10 s.

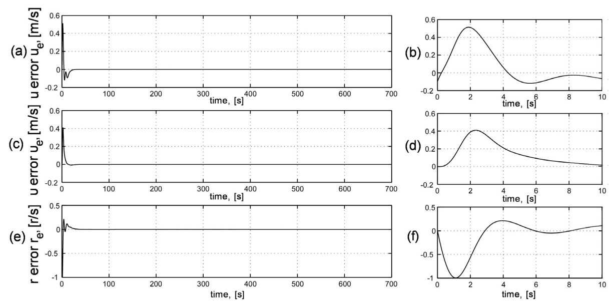

Fig. 5. (a), (c) Linear velocity tracking errors. (b), (d) First 10 s.

(e) Angular velocity tracking error. (f) First 10 s.

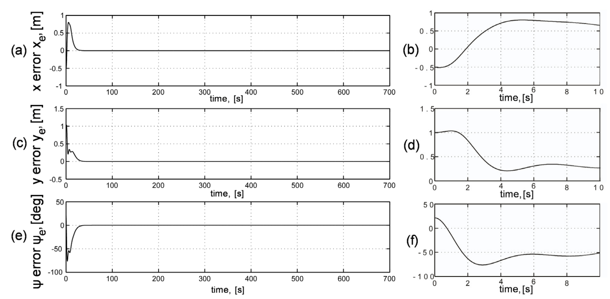

Fig. 6. (a), (c) Position tracking errors. (b), (d) First 10 s.

(e) Orientation tracking error. (f) First 10 s.

In order to investigate the effects of measurement noise on system performance, additional simulations were carried out in which white noise was injected in all measurements and the propagation of noise was studied. It was found that due to the structure of the controller, significant noise is present in the actuator command signals. However, the AUV dynamics filter the noise and the tracking errors still converge to a small bounded set of zero with very little noise. To further reduce the effect of noise, low-pass filters at the measurement channels or low-noise sensors can be employed.

V. Conclusions

In this paper, the combined problem of trajectory planning and tracking control for an underactuated AUV moving on the horizontal plane was addressed. The reference trajectory, consisting of the desired inertial position and the corresponding velocities, was designed to be a feasible "state-space" trajectory i.e. consistent with the vehicle dynamics. Based on the dynamics and the reference velocities, the reference orientation is also computed. Using the reference states and the vehicle states, the system dynamics was transformed to the error dynamics. Design methods such as partial state-feedback linearization, backstepping and nonlinear damping were used to force the tracking error to a small neighborhood of the origin that can be reduced arbitrarily. Computer simulations showed the validity of the designed trajectory planning and tracking control scheme.

References

[1] Yuh, J., "Design and Control of Autonomous Underwater Robots: A Survey", *Int. J. Control,* No 8, 2000, pp. 7-24.

[2] Fossen, T. I., *Guidance and Control of Ocean Vehicles,* New York: Wiley, 1994.

[3] Khalil, H. K., *Nonlinear Systems,* 2nd ed, Prentice Hall, Upper Saddle River, 1996.

[4] Aguiar, A. P., and Pascoal, A. M., "Dynamic Positioning and Way-Point Tracking of Underactuated AUVs in the presence of Ocean Currents", *Pr. 41st IEEE Conf. Dec. Con.,* Dec. 2002, pp. 2105-2110.

[5] Wichlund, K. Y., Sordalen, O., and Egeland, O., "Control Properties of Underactuated Vehicles", *Proc. IEEE Int. Conf. on Robotics and Automation,* May 1995, pp. 2009-2014.

[6] Reyhanoglou, M., "Exponential Stabilization of an Underactuated Autonomous Surface Vessel", *Automatica,* 33:12, 1997, pp. 2249-2254.

[7] Pettersen, K. Y., and Egeland, O., "Time-Varying Exponential Stabilization of the Position and Attitude of an Underactuated Autonomous Underwater Vehicle", *IEEE Transactions on Automatic Control,* Vol. 44, No 1, January 1999, pp. 112-115.

[8] Pettersen, K. Y., and Fossen, T. I., "Underactuated Dynamic Positioning of a Ship – Experimantal Results", *IEEE Transactions on Control Systems Technology,* 8:5, September 2000, pp. 856-863.

[9] Mazenc, F., Pettersen, K. Y., and Nijmeijer, H., "Global Uniform Asymptotic Stabilization of an Underactuated Surface Vessel", *IEEE Transactions on Automatic Control,* 47:10, October 2002, pp. 1759-1762.

[10] Kaminer, I., Pascoal, A., Hallberg, E., and Silvestre, C., "Trajectory Tracking for Autonomous Vehicles: An Integrated Approach to Guidance and Control", *J. Guidance, Control and Dynamics,* Vol. 21, No 1, January–February 1998, pp. 29-38.

[11] Pettersen, K. Y., and Nijmeijer, H., "Underactuated Ship Tracking Control: Theory and Experiments", *Int. J. Control,* Vol. 74, No 14, 2001, pp. 1435-1446.

[12] Lefeber, E., Pettersen, K. Y., and Nijmeijer, H., "Tracking Control of an Underactuated Ship", *IEEE Transactions on Control Systems Technology,* Vol. 11, No 1, January 2003, pp. 52-61.

[13] Jiang, Z. P., "Global Tracking Control of Underactuated Ships by Lyapunov's Direct Method", *Automatica,* 38:1, 2002, pp.301-309.

[14] Behal, A., Dawson, D. M., Dixon, W. E., and Fang, Y., "Tracking and Regulation Control of an Underactuated Surface Vessel with Nonintegrable Dynamics", *IEEE Transactions on Automatic Control,* Vol. 47, No 3, March 2002, pp. 495-500.

[15] Aguiar, P. A., and Hespanha, J. P., "Position Tracking of Underactuated Vehicles", *Pr. ACC,* June 2003.

[16] Krstic, M., Kanellakopoulos, I., and Kokotovic, P., *Nonlinear and Adaptive Control Design,* New York: Wiley, 1995.